© 2018. Published by The Company of Biologists Ltd | Journal of Experimental Biology (2018) 221, jeb183129. doi:10.1242/jeb.183129

RESEARCH ARTICLE

Physiological responses of ionotropic histamine receptors, PxHCLA and PxHCLB, to neurotransmitter candidates in a butterfly, *Papilio xuthus*

Hiroshi D. Akashi[1], Pei-Ju Chen[1], Tokiho Akiyama[1], Yohey Terai[1], Motohiro Wakakuwa[1], Yasunori Takayama[2,3], Makoto Tominaga[2,3] and Kentaro Arikawa[1,*]

ABSTRACT

Histamine is the only known neurotransmitter released by arthropod photoreceptors. Synaptic transmission from photoreceptors to second-order neurons is mediated by the activation of histamine-gated chloride channels (HCLs). These histaminergic synapses have been assumed to be conserved among insect visual systems. However, our understanding of the channels in question has thus far been based on studies in flies. In the butterfly *Papilio xuthus*, we have identified two candidate histamine-gated chloride channels, PxHCLA and PxHCLB, and studied their physiological properties using a whole-cell patch-clamp technique. We studied the responses of channels expressed in cultured cells to histamine as well as to other neurotransmitter candidates, namely GABA, tyramine, serotonin, D-/L-glutamate and glycine. We found that histamine and GABA activated both PxHCLA and PxHCLB, while the other molecules did not. The sensitivity to histamine and GABA was consistently higher in PxHCLB than in PxHCLA. Interestingly, simultaneous application of histamine and GABA activated both PxHCLA and PxHCLB more strongly than either neurotransmitter individually; histamine and GABA may have synergistic effects on PxHCLs in the regions where they co-localize. Our results suggest that the physiological properties of the histamine receptors are basically conserved among insects, but that the response to GABA differs between butterflies and flies, implying variation in early visual processing among species.

KEY WORDS: Visual system, GABA, Chloride channel, Visual processing, Photoreceptor

INTRODUCTION

Insects perceive the visual world via photoreceptors in their compound eyes. Upon light stimulation, the photoreceptors depolarize through activation of TRP channels (Hardie and Franze, 2012), which in turn leads to the hyperpolarization of postsynaptic lamina (or large) monopolar cells (LMCs) in the first optic ganglion, the lamina. In flies, it has been well established that this sign-inverted synaptic transmission is mediated by histamine-gated chloride channels (HCLs) (Hardie, 1987, 1989; Sarthy, 1991). Histamine has been found in the photoreceptors of a number of species including horseshoe crabs, barnacles, cockroaches, locusts, moths and butterflies (Battelle et al., 1991; Callaway and Stuart, 1989; Hamanaka et al., 2012; Nässel et al., 1988; Simmons and Hardie, 1988; Skingsley et al., 1995), suggesting that it is evolutionarily conserved as the major transmitter of arthropod photoreceptors.

Two genes, *hclA* and *hclB*, respectively encoding HCL subunits HCLA and HCLB, have been identified in the fruit fly *Drosophila melanogaster* (Gengs et al., 2002; Gisselmann et al., 2002; Zheng et al., 2002). These channels belong to a superfamily of Cys-loop receptors, which are pentameric ligand-gated channels (Thompson et al., 2010). Each receptor is composed of five subunits, which form homomeric or possibly heteromeric receptors. In flies, HCLA and HCLB subunits appear to form a heteromer in co-transfected cells, but it is unclear whether this occurs naturally in the visual system (Gisselmann et al., 2004; Pantazis et al., 2008). In contrast, the expression of HCLA and HCLB homomers has been confirmed. HCLA exists in neurons postsynaptic to photoreceptors, while HCLB exists in glial cells in the lamina (Pantazis et al., 2008), and in the region of the medulla (the second optic ganglion) where long axons of some photoreceptors terminate (Schnaitmann et al., 2018). Electrophysiological analysis has demonstrated that HCLA homomers expressed on cultured cells exhibit similar channel properties to the histamine-gated chloride channels on isolated LMCs (Pantazis et al., 2008; Skingsley et al., 1995). Furthermore, electroretinography has revealed that *hclA* null mutants fail to produce fast transient components derived from LMCs (Pantazis et al., 2008). These studies suggest that the channels on the LMCs are HCLA homomers in *D. melanogaster*.

Although considerable evidence has accumulated for the functional role of HCLs in visual processing in flies, their visual system is in fact peculiar in many aspects. For example, the projection pattern of photoreceptor axons is unique. In the lamina, eight photoreceptors originating from seven neighboring ommatidia are bundled together with five LMCs to form a lamina cartridge, in a connection scheme known as neural superposition (Hardie, 1985). Six of the eight photoreceptors are short visual fibers (svfs) which terminate in the lamina and are presynaptic to LMCs. The other two photoreceptors make no synaptic contacts in the lamina and instead send their long axons directly to the medulla, where they terminate on their postsynaptic targets; these photoreceptors are termed long visual fibers (lvfs) (Hardie, 1985). No photoreceptors have lateral processes extending into neighboring lamina cartridges in flies (Rivera-Alba et al., 2011), which also appears to be a characteristic unique to this insect order. In moths and bees, for example, a single cartridge comprises photoreceptor axons from a single ommatidium, and these have

[1]Department of Evolutionary Studies of Biosystems, SOKENDAI (The Graduate University for Advanced Studies), Hayama, Kanagawa 240-0193, Japan. [2]Division of Cell Signaling, Okazaki Institute for Integrative Bioscience (National Institute for Physiological Sciences), National Institutes of Natural Sciences, 5-1 Higashiyama, Myodaiji, Okazaki, Aichi 444-8787, Japan. [3]Department of Physiological Sciences, SOKENDAI (The Graduate University for Advanced Studies), 5-1 Higashiyama, Myodaiji, Okazaki, Aichi 444-8787, Japan.

*Author for correspondence (arikawa@soken.ac.jp)

K.A., 0000-0002-4365-0762

Received 27 April 2018; Accepted 3 September 2018

Journal of Experimental Biology (2018) 221, jeb183129. doi:10.1242/jeb.183129

long lateral processes penetrating into neighboring cartridges, where they form specific neuronal circuits (Ribi, 1976; Stöckl et al., 2016). Such variations in the lamina circuitry strongly suggest that the visual processing in the lamina is variable between species, probably reflecting differences in their visual ecology (Greiner et al., 2005).

Accumulated evidence indicates that butterflies have spectrally complex eyes and sophisticated color vision. We have initiated a comprehensive investigation of the lamina of the Japanese yellow swallowtail butterfly, *Papilio xuthus*, which has a tetrachromatic visual system (Koshitaka et al., 2008), in order to understand how visual information processing has diverged among insects. In the present study, we focused on the physiological function of HCL channels in *P. xuthus*. We first identified and cloned cDNAs encoding PxHCLA and PxHCLB subunits, and analyzed their physiological properties by performing whole-cell patch-clamp recordings. As several neurotransmitter candidates have been detected in the lamina of *P. xuthus* (Hamanaka et al., 2012) and other insects (Kolodziejczyk et al., 2008; Raghu and Borst, 2011; Sinakevitch and Strausfeld, 2004) in addition to histamine, we also studied HCL responses to these molecules, namely GABA (γ-aminobutyric acid), tyramine, serotonin, D-/L-glutamate and glycine.

MATERIALS AND METHODS

Animals

We used spring-form adult Japanese yellow swallowtail butterflies, *Papilio xuthus* Linnaeus, of both sexes. The butterflies were taken from a laboratory culture derived from eggs laid by females caught around the SOKENDAI campus in Hayama, Kanagawa, Japan.

Identification of *PxhclA* and *PxhclB* cDNA sequences

Whole-head tissues were dissected and preserved in RNA*later* solution (Thermo Fisher Scientific, Waltham, MA, USA). Total RNA was extracted from head tissue using TRIzol reagent (Thermo Fisher Scientific), and used for first-strand cDNA synthesis by PrimeScript II 1st Strand Synthesis Kit (TaKaRa, Shiga, Japan). We retrieved the *P. xuthus PxhclA* and *PxhclB* predicted cDNA sequences from GenBank (http://www.ncbi.nlm.nih.gov/genbank/) by BLASTN search (Altschul et al., 1990) using *D. melanogaster hclA* and *hclB* as query sequences: *PxhclA*: XM_013313248 and *PxhclB*: XM_013319237, respectively. We then retrieved the 5′- and 3′-untranslated region (UTR) of these homolog sequences from PapilioBase (http://papilio.bio.titech.ac.jp/papilio.html) (Nishikawa et al., 2015). We designed primers for PCR on both UTR sequences as follows: *PxhclA*_F1 (5’-taaggcaaaaaacttcccgcgaac-3′) and *PxhclA*_R1 (5’-tgctaaatcgagactggaagag-3′); and *PxhclB*_F1 (5′-ct-tgtgtgcgcgattgtacagtgac-3′) and *PxhclB*_R1 (5′-gttccacgag-tattggttttcatc-3′). We used these primer pairs to amplify the *PxhclA* and *PxhclB* full-length cDNAs by PCR using Ex Taq HS polymerase (TaKaRa). Reactions for the cDNA amplifications were carried out in a Mastercycler (Eppendorf, Hamburg, Germany) using the following protocol: an initial denaturing step at 93°C for 3 min, 30 cycles of denaturation at 93°C for 1 min, annealing at 60° C for 1 min, extension at 72°C for 1 min 35 s, and a final extension

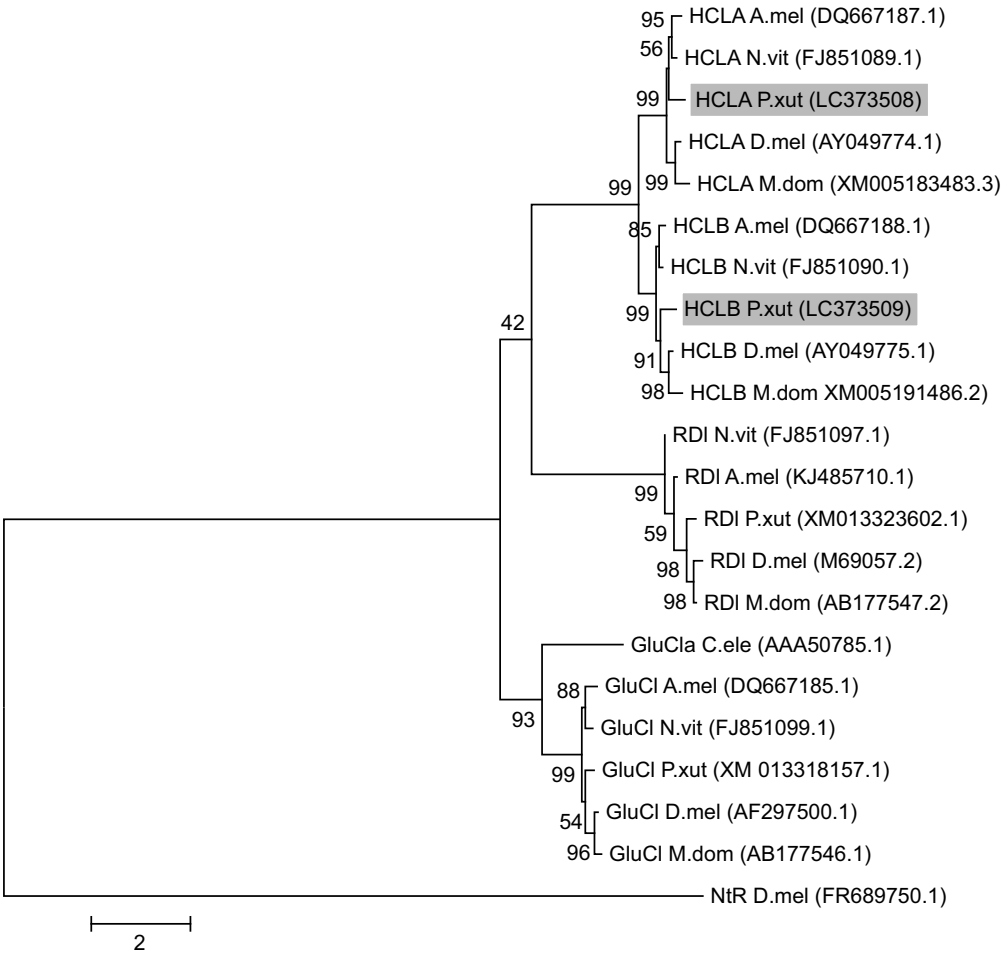

Fig. 1. Maximum likelihood tree showing relationships between Cys-loop chloride channel subunit nucleotide sequences of *Apis mellifera*, *Nasonia vitripennis*, *Drosophila melanogaster*, *Musca domestica* and *Papilio xuthus*. Gray boxes highlight PxHCLA and PxHCLB, which were determined in this study, and the tree indicates that these sequences are likely to be HCLA and HCLB homologs. Bootstrap values with 1000 replicates are shown at each node, and the scale bar indicates two changes per nucleotide. *Caenorhabditis elegans* glutamate-gated chloride channel is included in the tree for reference, to deduce the domains and structures particular to Cys-loop chloride channels. *Drosophila melanogaster* nicotinic acetylcholine receptor is included as an outgroup. Accession numbers for each sequence are shown in parentheses. HCLA, histamine-gated chloride channel subunit A; HCLB, histamine-gated chloride channel subunit B; RDI, resistant-to-dieldrin or GABA (gamma-aminobutyric acid)-activated chloride-selective receptor; GluCla, glutamate-gated chloride channel alpha; GluCl, glutamate-gated chloride channel; NtR, nicotinic acetylcholine receptor; A.mel, *Apis mellifera*; N.vit, *Nasonia vitripennis*; D.mel, *Drosophila melanogaster*; M.dom, *Musca domestica*; P.xut, *Papilio Xuthus*; C.ele, *Caenorhabditis elegans*.

Journal of Experimental Biology (2018) 221, jeb183129. doi:10.1242/jeb.183129

step at 72°C for 1 min. DNA sequencing was performed for the purified PCR products using BigDye Terminator v3.1 Cycle Sequencing Kit (Applied Biosystems, Foster City, CA, USA) with the PCR primers or inner primers: *PxhclA*_seqF1 (5′-gacatttt-cttcgcccaaacgtg-3′) and *PxhclA*_seqR1 (5′-caggacatgatgacgatga-gac-3′); and *PxhclB*_seqF1 (5′-actttccacgagatgagcatacc-3′) and *PxhclB*_seqR1 (5′-ccaaagtaagcaacgatgtgac-3′). The sequences were analyzed using an ABI3130xl DNA Sequencer (Applied Biosystems). The *PxhclA* and *PxhclB* sequences determined in this study were deposited in the international nucleotide sequence database DDBJ (accession numbers LC373508 and LC373509, respectively).

Sequence analysis of *PxhclA* and *PxhclB*

We obtained coding sequences of the following molecules from GenBank: Cys-loop chloride channel subunits in *Apis mellifera*, *Nasonia vitripennis*, *D. melanogaster*, *Musca domestica* and *P. xuthus*; glutamate-gated chloride channel in *Caenorhabditis elegans*; nicotinic acetylcholine receptor of *D. melanogaster*. The accession numbers of these sequences are shown in Figs 1 and 2. We translated these sequences and constructed the multiple protein sequence alignments with ClustalW (Thompson et al., 1994), using a gap-opening penalty and a gap-extension penalty of 3 and 1.8, respectively, with the Gonnet 250 protein weight matrix. For phylogenetic analysis, we converted the aligned amino acid sequences back to nucleotide sequences. In MEGA7 (Kumar et al., 2016), we inferred a phylogenetic tree from the alignment by using the Maximum Likelihood method based on the General Time Reversible model of sequence evolution with gamma distributed rates and 1000 bootstrap replicates. All positions containing gaps were eliminated, resulting in a total of 990 positions in the final dataset for the analysis. The tree is scaled with branch lengths measured in the number of substitutions per site. Nicotinic acetylcholine receptor of *D. melanogaster* was used as the outgroup.

Vector construction

We designed primers *PxhclA*_F1_IF (5′-taccgagctcggatctaagg-caaaaaacttcccgcgaac-3′) and *PxhclA*_R1_IF (5′-cacactggactagtgtgc-taaatcgagactggaagag-3′); and *PxhclB*_F1_IF (5′-taccgagctcggatccttgt gtgcgcgattgtacagtgac-3′) and *PxhclB*_R1_IF (5′-cacactggactagtggtt ccacgagtattggttttcatc-3′); the 15 bases at 5′ end of these primers overlapped with the ends of the cloning site of the linearized vector for cloning. We used these primers to amplify the cDNA containing the entire coding region of *PxhclA* or *PxhclB* by PCR using PrimeSTAR Max DNA polymerase (TaKaRa). Reactions for the cDNA amplifications were carried out in Mastercycler (Eppendorf) using the following protocol: an initial denaturing step at 98°C for 3 min, 30 cycles of denaturation at 98°C for 10 s, annealing at 55°C for 15 s, extension at 72°C for 2 min and a final extension step at 72°C for 1 min. After purification of the PCR products, we independently subcloned each cDNA (*PxhclA* and *PxhclB*) into the pcDNA3.1(+) vector (Invitrogen, Carlsbad, CA, USA) using the In-Fusion HD Cloning Kit (TaKaRa). The plasmids were transformed into *ECOS* competent *E. coli* DH5α cells (Nippon Gene, Tokyo, Japan). Each *E. coli* cell with plasmid clone was grown in 2 ml of LB medium supplemented with ampicillin overnight. The plasmid DNAs were purified from the culture using QIAprep Spin Miniprep Kit (Qiagen, Germantown, MD, USA). We confirmed the target insert sequences by PCR and sequencing.

Cell transfection

We transfected HEK293 cells with pGL1 vector (0.1 µg) and the pcDNA3.1(+)-*PxhclA* vector (1 µg), the pcDNA3.1(+)-*PxhclB* vector (1 µg), both vectors (0.5 µg each) or neither (as the control) in OPTI-MEM medium (Life Technologies) using Lipofectamine Plus reagents (Life Technologies). After 3 h of incubation at 37°C, we replaced the OPTI-MEM medium with D-MEM medium (Life Technologies), and the cells were settled and cultured on 12 mm-diameter coverslips at 37°C. We thus obtained four types

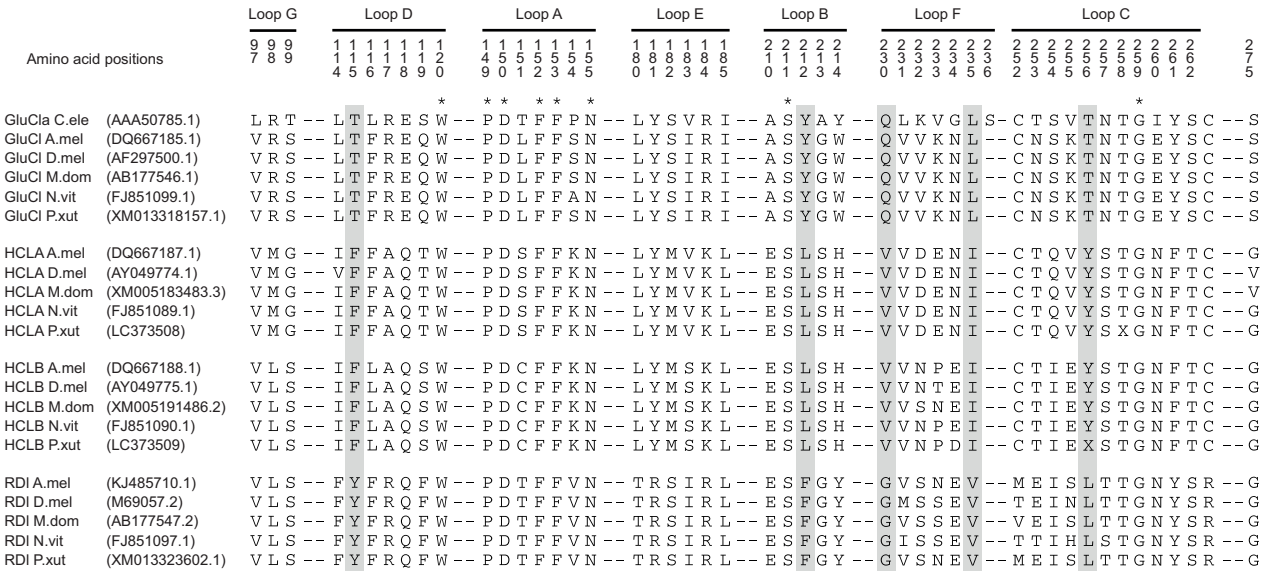

Fig. 2. Alignment of amino acid sequences of loop structures containing putative agonist binding sites. The residues are deduced from the alignments to *C. elegans* GluCla, the 3D structure of which has been determined (Hibbs and Gouaux, 2011). Asterisks indicate conserved sites across all molecules. Gray boxes indicate the sites that differ among the channels in a manner reflecting their specific agonists. Accession numbers for each sequence are shown in parentheses. Sequences between loops are omitted from the figure and represented by hyphens. The number of hyphens does not indicate the length of the sequences omitted. GluCla, glutamate-gated chloride channel alpha; GluCl, glutamate-gated chloride channel; HCLA, histamine-gated chloride channel subunit A; HCLB, histamine-gated chloride channel subunit B; RDI, resistant-to-dieldrin and GABA-activated chloride-selective receptor; C.ele, *Caenorhabditis elegans*; A.mel, *Apis mellifera*; D.mel, *Drosophila melanogaster*; M.dom, *Musca domestica*; N.vit, *Nasonia vitripennis*; P.xut, *Papilio xuthus*.

Journal of Experimental Biology (2018) 221, jeb183129. doi:10.1242/jeb.183129

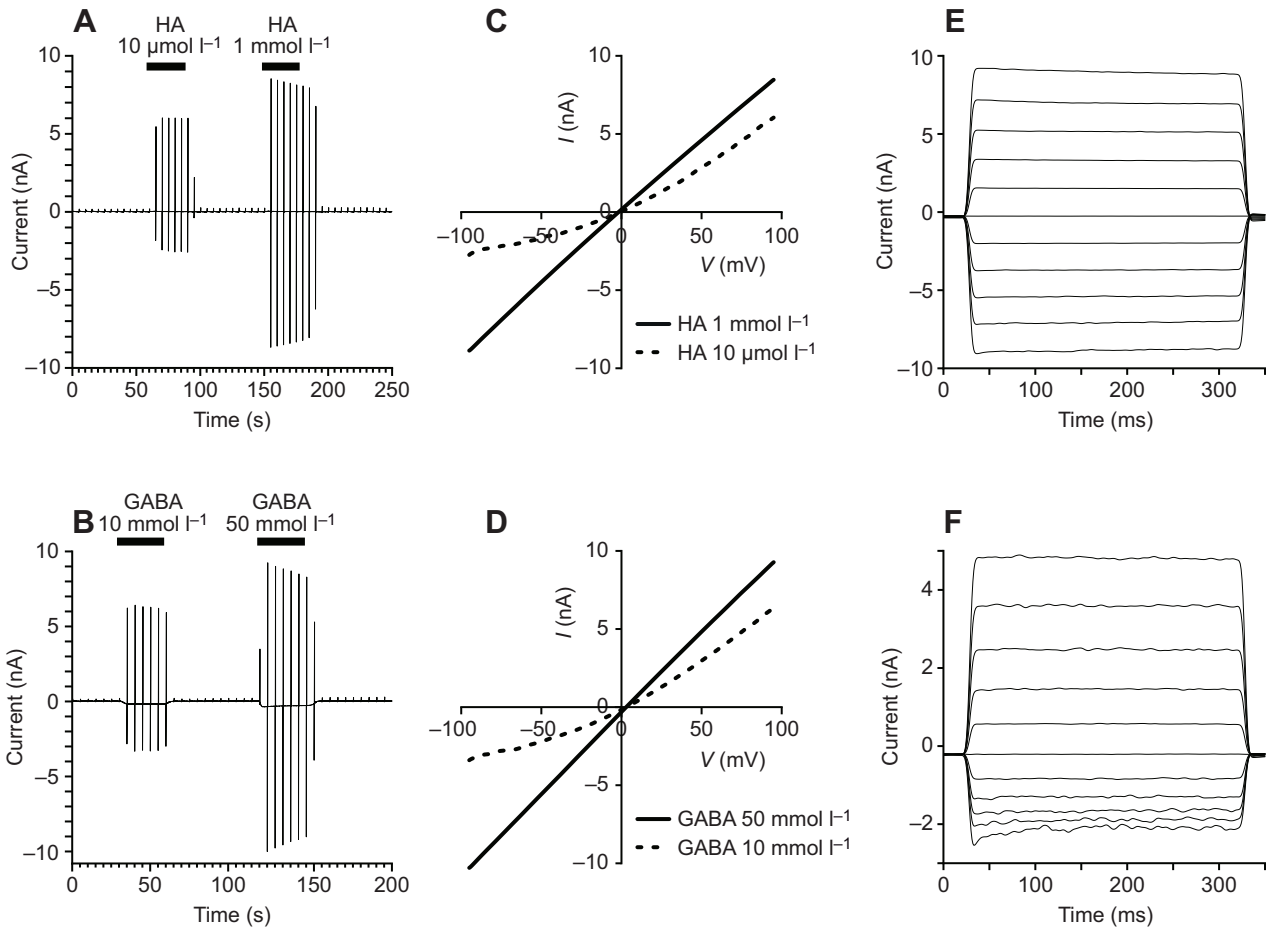

Fig. 3. Representative current traces of PxHCLA expressed in HEK293 cells under histamine and GABA application. (A,B) Representative current traces showing activation of PxHCLA by histamine (HA: 10 µmol l^{-1} and 1 mmol l^{-1}; A) and GABA (10 and 50 mmol l^{-1}; B) in a dose-dependent manner. Bars indicate the duration of chemical application. (C,D) Current–voltage (*I*–*V*) relationship for PxHCLA at two HA (C) and GABA (D) concentrations. A linear relationship exists at high histamine and GABA concentrations but weak rectification is observed at low concentrations. (E,F) Representative traces of current through PxHCLA recorded under 20 µmol l^{-1} HA (E) and 10 mmol l^{-1} GABA (F) during 300 ms voltage steps between −100 mV and +100 mV with an increment of 20 mV. Currents were stable over 300 ms at all voltages.

of cells expressing PxHCLA homomer, PxHCLB homomer, a combination of the two, i.e. PxHCLA/B, or neither of them. We carried out more than 30 independent transfections throughout the study.

Electrophysiological recordings

We performed whole-cell patch-clamp recordings as described previously (Takayama et al., 2017). A coverslip with cultured cells on the top was placed in the chamber mounted on a Nikon Eclipse TE2000-S inverted microscope. Standard bath solution for the whole-cell patch-clamp recording contained (in mmol l^{-1}); 140 NaCl, 5 KCl, 2 $CaCl_2$, 2 $MgCl_2$, 10 glucose and 10 Hepes. This solution was also used as a vehicle for chemicals (histamine, GABA, tyramine, serotonin, L-/D-glutamate and glycine) tested in the following experiments. The bath solutions were maintained at about 26°C, and perfused through silicone tubes by gravity. The solution in the pipette used for the whole-cell patch-clamp recording contained (in mmol l^{-1}): 140 KCl, 5 EGTA and 10 Hepes. The pH of all solutions was adjusted to 7.4 by NaOH. The whole-cell recording data were collected at a sampling frequency of 10 kHz and low-pass filtered with a cut-off of 5 kHz for analysis (Axopatch 200B Amplifier, Molecular Devices), which was performed using pCLAMP 10.4 software (Molecular Devices). For the experiments analyzing the responses of PxHCLs to agonists, voltage-ramp pulses (300 ms duration) from −100 to +100 mV were applied every 5 s to the patch-clamped cell, which was held at 0 mV. To test current stability during the 300 ms of voltage-ramp pulses, voltage-step pulses (300 ms) from −100 mV to +100 mV with an increment of 20 mV were applied to the patch-clamped cell held at 0 mV every 60 s to obtain a stable base line. Whole-cell patch-clamp recordings were performed 16–22 h after transfection of HEK293 cells. All of the patch-clamp experiments were performed at room temperature.

Statistical analysis

We obtained the current responses at −60 mV in the voltage-ramp pulses for analysis. To analyze the histamine and GABA dose dependency of PxHCLs, the current responses were normalized to the maximal current response (I/I_{max}). We used these normalized currents to draw dose–response curves by fitting the data using the simple Hill function:

$$\frac{I}{I_{max}} = \frac{1}{1 + ((EC_{50})/([\text{agonist}]))^{n_H}}, \quad (1)$$

where EC_{50} represents the concentration of histamine or GABA required to elicit 50% of I_{max}, 'agonist' is either histamine or GABA, and n_H represents the Hill coefficient. To analyze the effects

Journal of Experimental Biology (2018) 221, jeb183129. doi:10.1242/jeb.183129

of histamine and GABA on PxHCLs, the current responses elicited by the initial histamine application were used to normalize the subsequent current responses. We avoided using a saturating concentration of histamine to reduce the risks of cell damage for the later chemical applications. Statistical significance was evaluated using Student's paired *t*-test at a value of $P<0.05$. Data in figures are presented as means±s.e.m.

RESULTS

Molecular phylogeny

We determined the full-length sequences of cDNAs encoding PxHCLA (378 amino acids) and PxHCLB (427 amino acids). The phylogenetic analysis of Cys-loop chloride channels including these sequences showed that they were clustered according to their specific ligands (Fig. 1). Agonists are thought to bind at the interfaces between adjacent receptor subunits (Hibbs and Gouaux, 2011; Karlin, 2002; Sine, 2002). As the 3D structure of the glutamate-gated chloride channel has been determined in *C. elegans* (Hibbs and Gouaux, 2011), we used this sequence as a reference to deduce the agonist binding sites, or loop A–G, of Cys-loop chloride channels. The amino acid sequences at the putative agonist binding sites are highly conserved, particularly for the loop A structure (Fig. 2). Of the seven amino acids that comprise loop A, five are identical across all analyzed channels. In addition, we detected five sites (gray boxes in Fig. 2) that are more or less specific to the receptors' agonists. For example, the amino acid at position 115 in loop D is threonine for glutamate receptors, phenylalanine for histamine receptors and tyrosine for GABA receptors.

Physiology

During the 16–22 h period after transfection, whole-cell currents could be recorded upon application of histamine and GABA to the cells transfected with *PxhclA*, *PxhclB* or both. We could not detect any currents from cells with other tested chemicals (tyramine, serotonin, L-/D-glutamate and glycine). In control cells, no responses were recorded to any chemicals, including histamine and GABA.

Fig. 3A,B shows representative current traces recorded from *PxhclA* transfected cells under histamine and GABA application, respectively. Fig. 3C,D shows the current–voltage (*I–V*) relationship of *PxhclA* transfected cells under the application of histamine and GABA, respectively. The *I–V* relationship was basically linear at higher concentrations, but weak outward rectification was observed at lower concentrations. As the intracellular and extracellular concentrations of chloride ions were approximately equal in our experiments, this implies a reversal potential for chloride ions of around 0 mV, which was consistent with our results (Fig. 3C,D). The voltage-step pulses produced

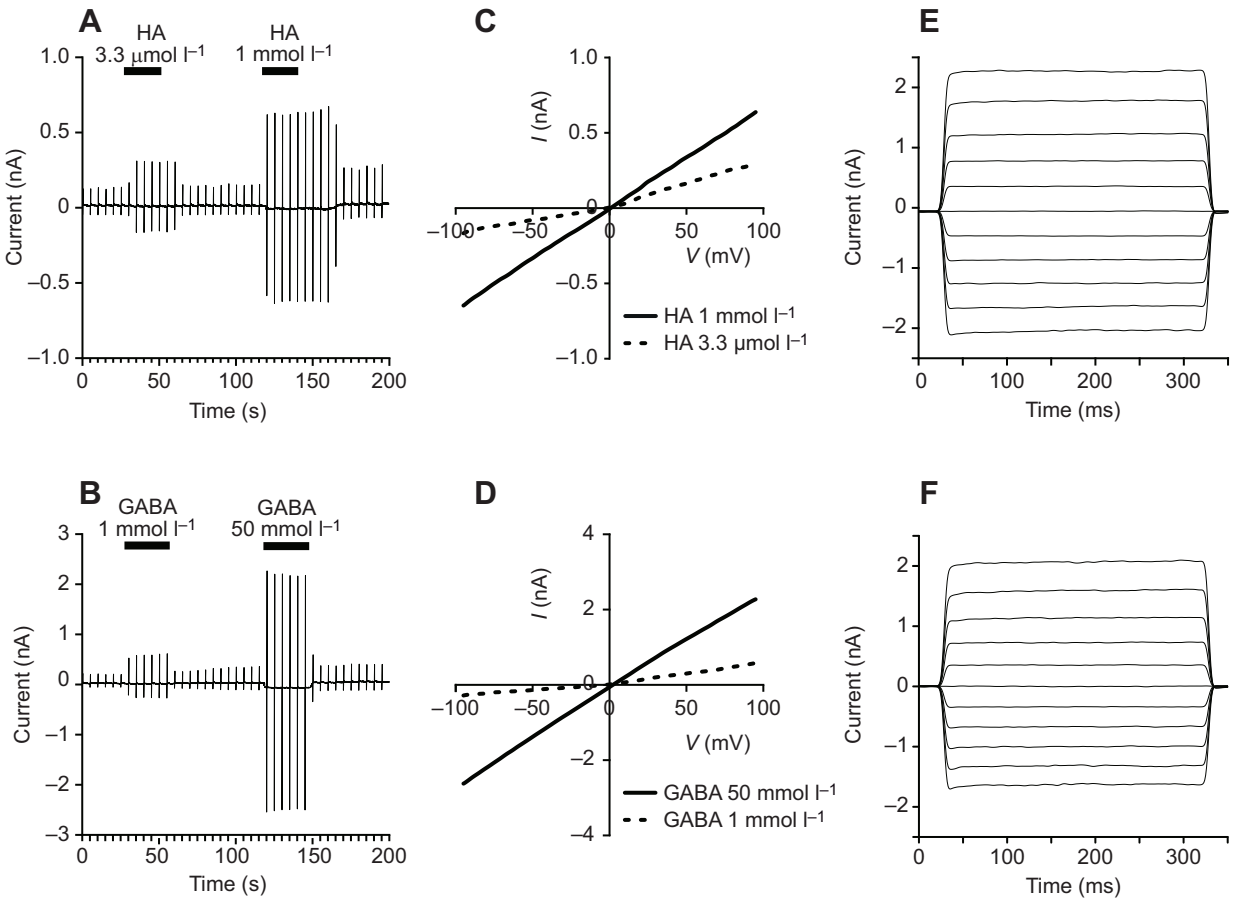

Fig. 4. Representative current traces of PxHCLB expressed in HEK293 cells under histamine and GABA application. (A,B) Representative current traces showing activation of PxHCLB by histamine (HA: 3.3 µmol l^{-1} and 1 mmol l^{-1}; A) and GABA (1 and 50 mmol l^{-1}; B) in a dose-dependent manner. Bars indicate the duration of chemical application. (C,D) *I–V* relationship of PxHCLB at two HA (C) and GABA (D) concentrations. A linear relationship exists at high histamine and GABA concentrations but weak rectification is observed at low concentrations. (E,F) Representative traces of current through PxHCLB recorded under 6.6 µmol l^{-1} HA (E) and 2.5 mmol l^{-1} GABA (F) during 300 ms voltage steps between −100 mV and +100 mV with an increment of 20 mV. Currents were stable over 300 ms at all voltages.

Journal of Experimental Biology (2018) 221, jeb183129. doi:10.1242/jeb.183129

histamine and GABA-induced currents that were stable over a 300 ms interval (Fig. 3E,F).

Fig. 4 shows the results obtained from analysis of *PxhclB* transfected cells under histamine and GABA application, in the same format as Fig. 3 for *PxhclA* transfected cells. While we observed dose-dependent responses in *PxhclB* transfected cells, as for *PxhclA* transfected cells, the maximal current responses were generally smaller in the former than the latter (see scales of Figs 3 and 4). *PxhclB* transfected cells showed a linear *I–V* relationship at high agonist concentrations but weak outward rectification at low concentrations (Fig. 4C,D). Histamine- and GABA-induced currents were stable over 300 ms (Fig. 4E,F).

Fig. 5 shows histamine and GABA dose dependency fitted with the simple Hill function for cells transfected by *PxhclA*, *PxhclB* or both. The fitted parameters of EC_{50} and the slope, n_H, are summarized in Table 1. *PxhclB* transfected cells showed the highest sensitivity to both histamine and GABA. For both histamine and GABA, the slope of the dose–response curves was shallowest for *PxhclA*/*PxhclB* co-transfected cells, while the slopes were similar between *PxhclA* and *PxhclB* transfected cells. We used 1 mmol l^{-1} histamine and 50 mmol l^{-1} GABA across all three transfections to obtain their maximal current responses for each agonist. However, the currents recorded from those cells reached their maxima at lower agonist concentrations. According to the dose–response curves, the saturating concentrations of histamine were, in fact, approximately 300 µmol l^{-1} and 30 µmol l^{-1} for *PxhclA* and *PxhclB* transfected cells, respectively, and that of GABA was 10 mmol l^{-1} for *PxhclB* transfected cells (Fig. 5).

Simultaneous application of histamine and GABA elicited synergistic effects. Fig. 6A–C shows representative response traces of *PxhclA* transfected, *PxhclB* transfected and *PxhclA*/*PxhclB* co-transfected cells, respectively. The sum of the current responses elicited from individual application of histamine and GABA was significantly smaller than the current responses elicited from histamine and GABA mixtures in all transfection cases (Fig. 6D–F).

Note that we used HEK293 cells to express the molecules. Physiological responses of ectopically expressed HCLs of *D. melanogaster* and *M. domestica* were analyzed using insect S2 cells (Pantazis et al., 2008) and *Xenopus* oocytes (Kita et al., 2017), respectively. These studies including our present one have revealed similar characteristics, indicating that the effect of using different expression systems would be minimal.

DISCUSSION

Molecular characteristics

Phylogenetic analysis suggests *PxhclA* and *PxhclB* genes are homologs of other insects' *hcl* genes as they cluster according to their specific ligands (Fig. 1). The amino acid sequences in putative agonist binding sites provide some candidate residues in loop B, C, D and F for determining agonist specificity among Cys-loop chloride channels (Fig. 2). In *D. melanogaster* and *M. domestica*, histamine activates all HCL conformations, but GABA only activates HCLB homomers (Gisselmann et al., 2004; Kita et al., 2017). Interestingly, both histamine and GABA activate all HCL conformations in *Papilio*. Although the GABA-mediated activation mechanism in HCLs remains unknown, we found one amino acid residue that distinguishes the subunits capable of binding GABA, such as PxHCLA, PxHCLB, fly HCLB and RDls (resistant-to-dieldrin or GABA-activated chloride-selective receptors), from the

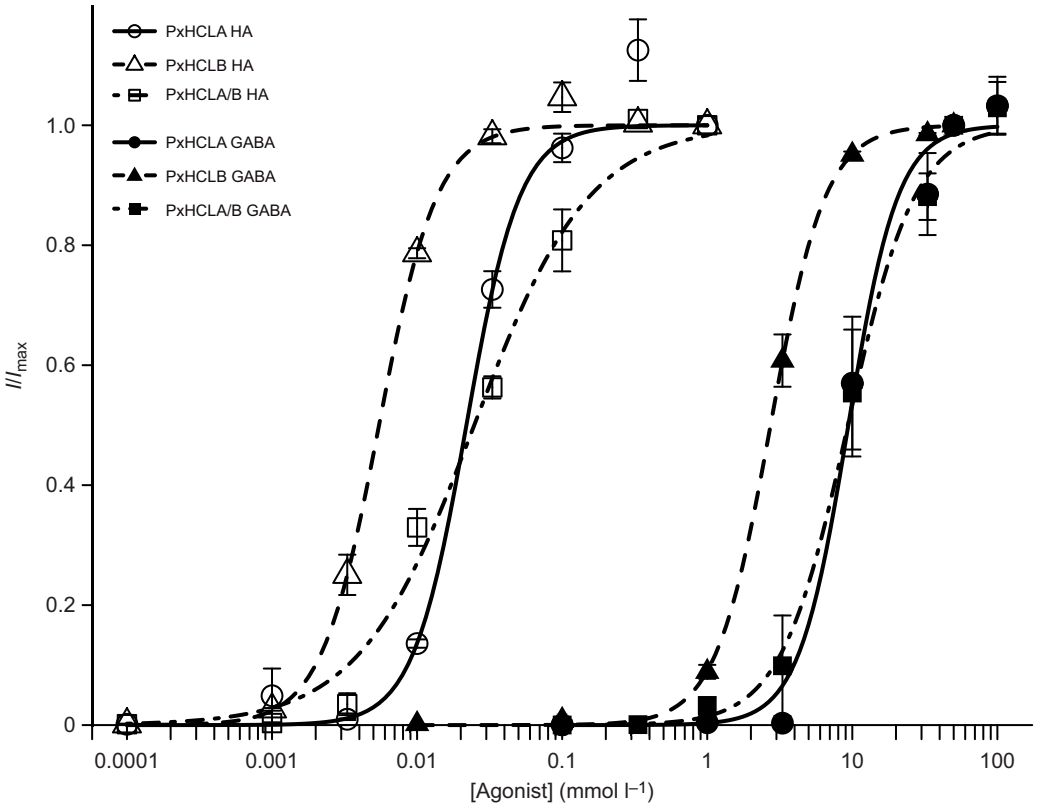

Fig. 5. Dose–response curves of PxHCLA, PxHCLB and PxHCLA/B for histamine and GABA. Current amplitudes were normalized by the current at 1 mmol l^{-1} (I/I_{max}) for histamine (HA) and 50 mmol l^{-1} for GABA. Each point is based on the measurement from at least three separate cells taken from six independent transfection sessions in total. The curves were drawn by simple Hill fittings (Eqn 1).

Journal of Experimental Biology (2018) 221, jeb183129. doi:10.1242/jeb.183129

Table 1. Histamine and GABA dose–response parameters of PxHCLs

	Histamine		GABA	
Receptor type	EC_{50} (μmol l^{-1})	n_H	EC_{50} (mmol l^{-1})	n_H
PxHCLA homomer	21.9±1.6	2.4±0.3	9.4±0.8	2.5±0.7
PxHCLB homomer	5.5±0.2	2.2±0.1	2.7±0.1	2.3±0.2
PxHCLA/B	24.8±2.9	1.1±0.1	9.3±0.9	1.9±0.3

All fitted parameters are means±s.e.m.

subunits capable of binding histamine only, such as fly HCLA. The residue is at position 275, which is outside of the putative agonist binding sites (Fig. 2; Fig. S1). The HCLs and RDls in Fig. 2 have glycine at this position except for the fly HCLA, which has valine there. This suggests that the mutation from glycine to valine at position 275 (G275V) caused the loss of function in the fly HCLA lineage. Further electrophysiological analysis on HCLs from bee lineages and HCLs with site-directed mutations would provide clues to understand the significance of amino acid substitutions for GABA binding.

Physiological properties and functional implications

Electrophysiological studies on HCLs in *D. melanogaster* and *M. domestica* have shown that the EC_{50} values of native channels on the LMCs for histamine (24 and 34 μmol l^{-1}, respectively) are similar to those of *in vitro*-expressed HCLA homomers for histamine (25 and 33 μmol l^{-1}, respectively) (Kita et al., 2017; Pantazis et al., 2008; Skingsley et al., 1995). As PxHCLA homomers have an EC_{50} for histamine (21.87 μmol l^{-1}) similar to that of *D. melanogaster*, PxHCLA homomers most likely have a similar biological function, i.e. synaptic transmission from photoreceptors to LMCs. In fact, PxHCLA is expressed in neurons postsynaptic to photoreceptors in both the lamina and the medulla of *P. xuthus* (Chen et al., 2016).

PxHCLB homomers have a much lower EC_{50} for histamine than PxHCLA homomers. Histamine at the concentration of the PxHCLB homomer EC_{50} barely activates PxHCLA, reaching only around 5% of its maximum current (Fig. 5). Although the lower EC_{50} for histamine of the HCLB homomer than of HCLA is consistent with previous reports in flies (Gisselmann et al., 2004; Kita et al., 2017), its significance remains unclear. Recently Schnaitmann et al. (2018) demonstrated in *D. melanogaster* that two lvfs (R7 and R8), originating from the same ommatidia, directly inhibit each other at their axon terminals in the medulla via HCLB, resulting in spectral opponency in these photoreceptors. The higher histamine sensitivity of HCLB would cause it to activate more quickly than HCLA, which would allow photoreceptors to pre-process each other's signals in this way before the information reached higher order neurons. We have detected PxHCLB at interphotoreceptor connections in the lamina and the medulla of

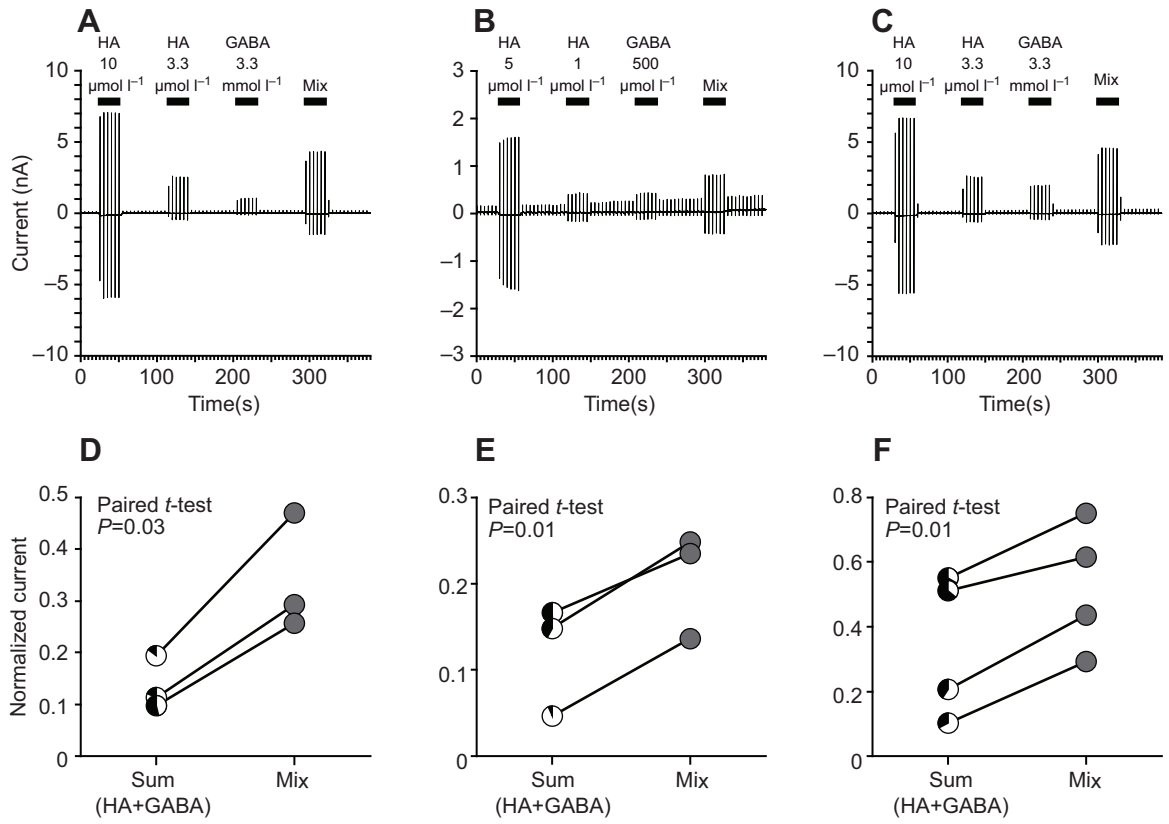

Fig. 6. Possible synergistic effects of histamine and GABA on PxHCLs. (A–C) Representative traces from HEK293 cell expressing PxHCLA (A), PxHCLB (B) and PxHCLA/B (C), showing the synergistic effects observed under histamine (HA) and GABA application. Bars indicate the duration of chemical applications. 'Mix' indicates the simultaneous application of histamine and GABA at concentrations equal to their concentrations on the second and third applications in the trial, respectively. (D–F) Synergistic effects of histamine and GABA on PxHCLA (D), PxHCLB (E) and PxHCLA/B (F). Lines connect responses recorded from the same cell. 'Sum' (HA+GABA) indicates the sum of the currents recorded from the second and third chemical applications. Pie charts indicate the ratio of histamine (white)- and GABA (black)-induced currents. 'Mix' indicates the currents recorded from the application of histamine and GABA mixtures (gray). Both sum and mix currents were normalized to the currents recorded from the first application of histamine.

P. xuthus (Chen et al., 2016), suggesting that they serve similar functions in butterflies.

For co-transfected cells, we observed partly discrepant results between *P. xuthus* and *D. melanogaster*. In *D. melanogaster*, *hclA*/*hclB* co-transfectants show the lowest EC_{50} for histamine among the three cell types (Gisselmann et al., 2004; Pantazis et al., 2008). In contrast, *PxhclA*/*PxhclB* co-transfectants have an EC_{50} for histamine similar to that of *PxhclA* transfected cells (Table 1). The EC_{50} of GABA in *PxhclA*/*PxhclB* co-transfectants is also similar to that of *PxhclA* transfectants. However, n_H, the slope of the histamine dose–response curve, was smaller in *PxhclA*/*PxhclB* co-transfectants than those of *PxhclA* and *PxhclB* transfectants, although the curve for GABA was pretty close to that of *PxhclA* transfectants. We need to carefully consider any possibilities of heteromeric channels and/or mixed expression of *PxhclA* and *PxhclB* homomers in the co-transfected cells in varying proportions. In fact, a shallower slope of the histamine dose–response curve has also been observed in the fly *hclA/hclB* co-transfectant (Pantazis et al., 2008); however, the underlying mechanism remains unclear. While HCLA has been localized in LMCs and medulla neurons, HCLB has been localized in lamina glial cells and lvfs R7 and R8 in *D. melanogaster* (Pantazis et al., 2008; Schnaitmann et al., 2018). Therefore, HCLA/B heteromers seem unlikely to exist *in vivo*, at least in the visual system.

In several experiments, we applied histamine and GABA simultaneously. We always found an increase in current upon co-application in all three transfectants (Fig. 6). This indicates the possibility that histamine and GABA might have synergistic effects on PxHCLs (Fig. 6), while simultaneous application of histamine and GABA affect HCLB of *M. domestica* only in an additive manner (Kita et al., 2017). The high sequence similarity between PxHCLs and fly HCLB, particularly in the putative agonist binding sites, implies that a small number of amino acid substitutions are responsible for the functional divergence, if any. The activation of PxHCLA or PxHCLB homomers by histamine and GABA might be functionally significant. In *P. xuthus*, for instance, a subset of LMCs are GABAergic (Hamanaka et al., 2012). They terminate in the distal region of the medulla along with the lvfs, which release histamine upon light stimulation. Thus, the possible synergistic effects of histamine and GABA could modulate synaptic transmission in this region.

The variability in the response to GABA between HCLA and PxHCLA may reflect differences in the underlying visual circuits between flies and butterflies. In flies, LMCs are postsynaptic to svfs R1–R6, which all have identical spectral sensitivity (Rivera-Alba et al., 2011), and they are assumed to be responsible mainly for motion vision. In contrast, the spectrally heterogeneous lvfs R7 and R8, which are thought to be essential for color vision, have no synaptic interactions with photoreceptors or LMCs in the lamina. Unlike in flies, the *Papilio* lvfs have a number of lateral processes in the lamina, making local contacts with both svfs and LMCs (Takemura and Arikawa, 2006). As a result, the medulla neurons expressing PxHCLA in *Papilio* receive not only chromatic inputs from histaminergic lvfs but also mixed chromatic and motion signals from LMCs, including GABAergic ones (Hamanaka et al., 2012). In contrast, the medulla neurons expressing HCLA in flies only receive chromatic signals from histaminergic lvfs because their HCLAs are insensitive to GABA. Therefore, we propose that flies have evolved an optimal achromatic motion vision system primarily dependent on R1–R6 broadband photoreceptors (Hardie, 1985), while in butterflies pathways for color and motion vision are less segregated at the early stages of visual processing (Stewart et al., 2015). We note that the sensitivity of PxHCLs to GABA is about 500-fold less than that of histamine. Whether or not this is physiologically relevant has to be confirmed, for example, by direct measurement of transmitter concentrations at the synaptic sites.

Skingsley et al. (1995) conducted whole-cell patch-clamp recordings on isolated LMCs in five dipteran species with diverse visual ecologies, in order to study the physiological characteristics of HCLA channels. The dose–response functions of LMCs in fast-flying diurnal species exhibit lower sensitivity (higher EC_{50} value) and a narrower dynamic range (larger n_H) than those in slow-flying crepuscular species. Under the histamine concentration that elicits 10% of I_{max} in each species, single-channel analyses of HCLAs have revealed similar properties between species. Therefore, the observed species differences should be attributed mainly to synaptic gain and perhaps also to the absolute sensitivity of single channels (Skingsley et al., 1995). To better understand the evolution of early visual processing in insects, it would be worthwhile to compare the LMC membrane response properties as well as single-channel properties, for example, between butterflies with flight speeds that differ greatly (Dudley and Srygley, 1994).

Acknowledgements
We thank Dr Finlay Stewart for critically reading the manuscript.

Competing interests
The authors declare no competing or financial interests.

Author contributions
Conceptualization: P.-J.C., K.A.; Methodology: Y. Takayama, M.T.; Formal analysis: H.D.A., P.-J.C., M.W., Y. Takayama; Investigation: H.D.A., P.-J.C., T.A., Y. Terai, M.W., Y. Takayama, K.A.; Data curation: H.D.A., T.A., Y. Terai, Y. Takayama, K.A.; Writing - original draft: H.D.A., K.A.; Writing - review & editing: H.D.A., P.-J.C., T.A., Y. Terai, M.W., Y. Takayama, M.T., K.A.; Supervision: Y. Takayama, M.T., K.A.; Project administration: K.A.; Funding acquisition: M.T., K.A.

Funding
This work was financially supported by Grants-in-Aid for Scientific Research (KAKENHI) from the Japan Society for the Promotion of Science (JSPS) to K.A. (26251036, 18H05273) and to P.-J.C. (16J07688). A major part of experiments was conducted under the collaborative research program of National Institute for Physiological Sciences.

Data availability
PxhclA and *PxhclB* sequences are deposited in DDBJ (accession numbers LC373508 and LC373509, respectively).

Supplementary information
Supplementary information available online at
http://jeb.biologists.org/lookup/doi/10.1242/jeb.183129.supplemental

References
Altschul, S. F., Gish, W., Miller, W., Myers, E. W. and Lipman, D. J. (1990). Basic local alignment search tool. *J. Mol. Biol.* **215**, 403-410.

Battelle, B.-A., Calman, B., Andrews, A., Grieco, F., Mleziva, M., Callaway, J. and Stuart, A. (1991). Histamine: a putative afferent neurotransmitter in *Limulus* eyes. *J. Comp. Neurol.* **305**, 527-542.

Callaway, J. C. and Stuart, A. E. (1989). Biochemical and physiological evidence that histamine is the transmitter of barnacle photoreceptors. *Vis. Neurosci.* **3**, 311-325.

Chen, P.-J., Matsushita, A. and Arikawa, K. (2016). Immunoelectron microscopic localization of histamine-gated chloride channels in the visual system of *Papilio xuthus*. In *The 37th Annual Meeting of the Taiwan Entomological Society*. Taipei.

Dudley, R. and Srygley, R. (1994). Flight physiology of neotropical butterflies: allometry of airspeeds during natural free flight. *J. Exp. Biol.* **191**, 125-139.

Gengs, C., Leung, H.-T., Skingsley, D. R., Iovchev, M. I., Yin, Z., Semenov, E. P., Burg, M. G., Hardie, R. C. and Pak, W. L. (2002). The target of *Drosophila* photoreceptor synaptic transmission is a histamine-gated chloride channel encoded by *ort* (*hclA*). *J. Biol. Chem.* **277**, 42113-42120.

Gisselmann, G., Pusch, H., Hovemann, B. T. and Hatt, H. (2002). Two cDNAs coding for histamine-gated ion channels in *D. melanogaster*. *Nat. Neurosci.* **5**, 11-12.

Gisselmann, G., Plonka, J., Pusch, H. and Hatt, H. (2004). Unusual functional properties of homo- and heteromultimeric histamine-gated chloride channels of *Drosophila melanogaster*: spontaneous currents and dual gating by GABA and histamine. *Neurosci. Lett.* **372**, 151-156.

Greiner, B., Ribi, W. A. and Warrant, E. J. (2005). A neural network to improve dim-light vision? Dendritic fields of first-order interneurons in the nocturnal bee *Megalopta genalis*. *Cell Tissue Res.*. **322**, 313-320.

Hamanaka, Y., Kinoshita, M., Homberg, U. and Arikawa, K. (2012). Immunocytochemical localization of amines and GABA in the optic lobe of the butterfly, *Papilio xuthus*. *PLoS ONE* **7**, e41109.

Hardie, R. C. (1985). Functional organization of the fly retina. In *Prog Sens Physiol*, Vol. 5 (ed. D. Ottoson), pp. 1-79. Berlin, Heidelberg, New York, Toronto: Springer.

Hardie, R. C. (1987). Is histamine a neurotransmitter in insect photoreceptors? *J. Comp. Physiol. A* **161**, 201-213.

Hardie, R. C. (1989). A histamine-activated chloride channel involved in neurotransmission at a photoreceptor synapse. *Nature* **339**, 704-706.

Hardie, R. C. and Franze, K. (2012). Photomechanical responses in *Drosophila* photoreceptors. *Science* **338**, 260-263.

Hibbs, R. E. and Gouaux, E. (2011). Principles of activation and permeation in an anion-selective Cys-loop receptor. *Nature* **474**, 54-60.

Karlin, A. (2002). Emerging structure of the nicotinic acetylcholine receptors. *Nature Rev. Neurosci.* **3**, 102-114.

Kita, T., Irie, T., Nomura, K., Ozoe, F. and Ozoe, Y. (2017). Pharmacological characterization of histamine-gated chloride channels from the housefly *Musca domestica*. *Neurotoxicology* **60**, 245-253.

Kolodziejczyk, A., Sun, X., Meinertzhagen, I. A. and Nässel, D. R. (2008). Glutamate, GABA and acetylcholine signaling components in the lamina of the *Drosophila* visual system. *PLoS ONE* **3**, e2110.

Koshitaka, H., Kinoshita, M., Vorobyev, M. and Arikawa, K. (2008). Tetrachromacy in a butterfly that has eight varieties of spectral receptors. *Proc. R. Soc. B* **275**, 947-954.

Kumar, S., Stecher, G. and Tamura, K. (2016). MEGA7: Molecular evolutionary genetics analysis version 7.0 for bigger datasets. *Mol. Biol. Evol.* **33**, 1870-1874.

Nässel, D. R., Holmqvist, M. H., Hardie, R. C., Håkanson, R. and Sundler, F. (1988). Histamine-like immunoreactivity in photoreceptors of the compound eyes and ocelli of the flies *Calliphora erythrocephala* and *Musca domestica*. *Cell Tissue Res.* **253**, 639-646.

Nishikawa, H., Iijima, T., Kajitani, R., Yamaguchi, J., Ando, T., Suzuki, Y., Sugano, S., Fujiyama, A., Kosugi, S. and Hirakawa, H. (2015). A genetic mechanism for female-limited Batesian mimicry in *Papilio* butterfly. *Nat. Genet.* **47**, 405-409.

Pantazis, A., Segaran, A., Liu, C.-H., Nikolaev, A., Rister, J., Thum, A. S., Roeder, T., Semenov, E., Juusola, M. and Hardie, R. C. (2008). Distinct roles for two histamine receptors (hclA and hclB) at the *Drosophila* photoreceptor synapse. *J. Neurosci.* **28**, 7250-7259.

Raghu, S. V. and Borst, A. (2011). Candidate glutamatergic neurons in the visual system of *Drosophila*. *PLoS ONE* **6**, e19472.

Ribi, W. A. (1976). The first optic ganglion of the bee. II. Topographical relationships of the monopolar cells within and between cartridges. *Cell Tissue Res.* **171**, 359-373.

Rivera-Alba, M., Vitaladevuni, S. N., Mishchenko, Y., Lu, Z., Takemura, S. Y., Scheffer, L., Meinertzhagen, I. A., Chklovskii, D. B. and de Polavieja, G. G. (2011). Wiring economy and volume exclusion determine neuronal placement in the *Drosophila* brain. *Curr. Biol.* **21**, 2000-2005.

Sarthy, P. V. (1991). Histamine: a neurotransmitter candidate for *Drosophila* photoreceptors. *J. Neurochem.* **57**, 1757-1768.

Schnaitmann, C., Haikala, V., Abraham, E., Oberhauser, V., Thestrup, T., Griesbeck, O. and Reiff, D. F. (2018). Color processing in the early visual system of *Drosophila*. *Cell* **172**, 318-330 e18.

Simmons, P. J. and Hardie, R. C. (1988). Evidence that histamine is a neurotransmitter of photo-receptors in the locust ocellus. *J. Exp. Biol.* **138**, 205-219.

Sinakevitch, I. and Strausfeld, N. J. (2004). Chemical neuroanatomy of the fly's movement detection pathway. *J. Comp. Neurol.* **468**, 6-23.

Sine, S. M. (2002). The nicotinic receptor ligand binding domain. *Dev. Neurobiol.* **53**, 431-446.

Skingsley, D., Laughlin, S. and Hardie, R. C. (1995). Properties of histamine-activated chloride channels in the large monopolar cells of the dipteran compound eye: a comparative study. *J. Comp. Physiol. A* **176**, 611-623.

Stewart, F. J., Kinoshita, M. and Arikawa, K. (2015). The butterfly *Papilio xuthus* detects visual motion using chromatic contrast. *Biol. Lett.* **11**, 20150687.

Stöckl, A. L., Ribi, W. A. and Warrant, E. J. (2016). Adaptations for nocturnal and diurnal vision in the hawkmoth lamina. *J. Comp. Neurol.* **524**, 160-175.

Takayama, Y., Furue, H. and Tominaga, M. (2017). 4-isopropylcyclohexanol has potential analgesic effects through the inhibition of anoctamin 1, TRPV1 and TRPA1 channel activities. *Sci. Rep.* **7**, 43132.

Takemura, S.-Y. and Arikawa, K. (2006). Ommatidial type-specific interphotoreceptor connections in the lamina of the swallowtail butterfly, *Papilio xuthus*. *J. Comp. Neurol.* **494**, 663-672.

Thompson, J. D., Higgins, D. G. and Gibson, T. J. (1994). CLUSTAL W: improving the sensitivity of progressive multiple sequence alignment through sequence weighting, position-specific gap penalties and weight matrix choice. *Nucleic Acids Res.* **22**, 4673-4680.

Thompson, A. J., Lester, H. A. and Lummis, S. C. (2010). The structural basis of function in Cys-loop receptors. *Q. Rev. Biol.* **43**, 449-499.

Zheng, Y., Hirschberg, B., Yuan, J., Wang, A. P., Hunt, D. C., Ludmerer, S. W., Schmatz, D. M. and Cully, D. F. (2002). Identification of two novel *Drosophila melanogaster* histamine-gated chloride channel subunits expressed in the eye. *J. Biol. Chem.* **277**, 2000-2005.